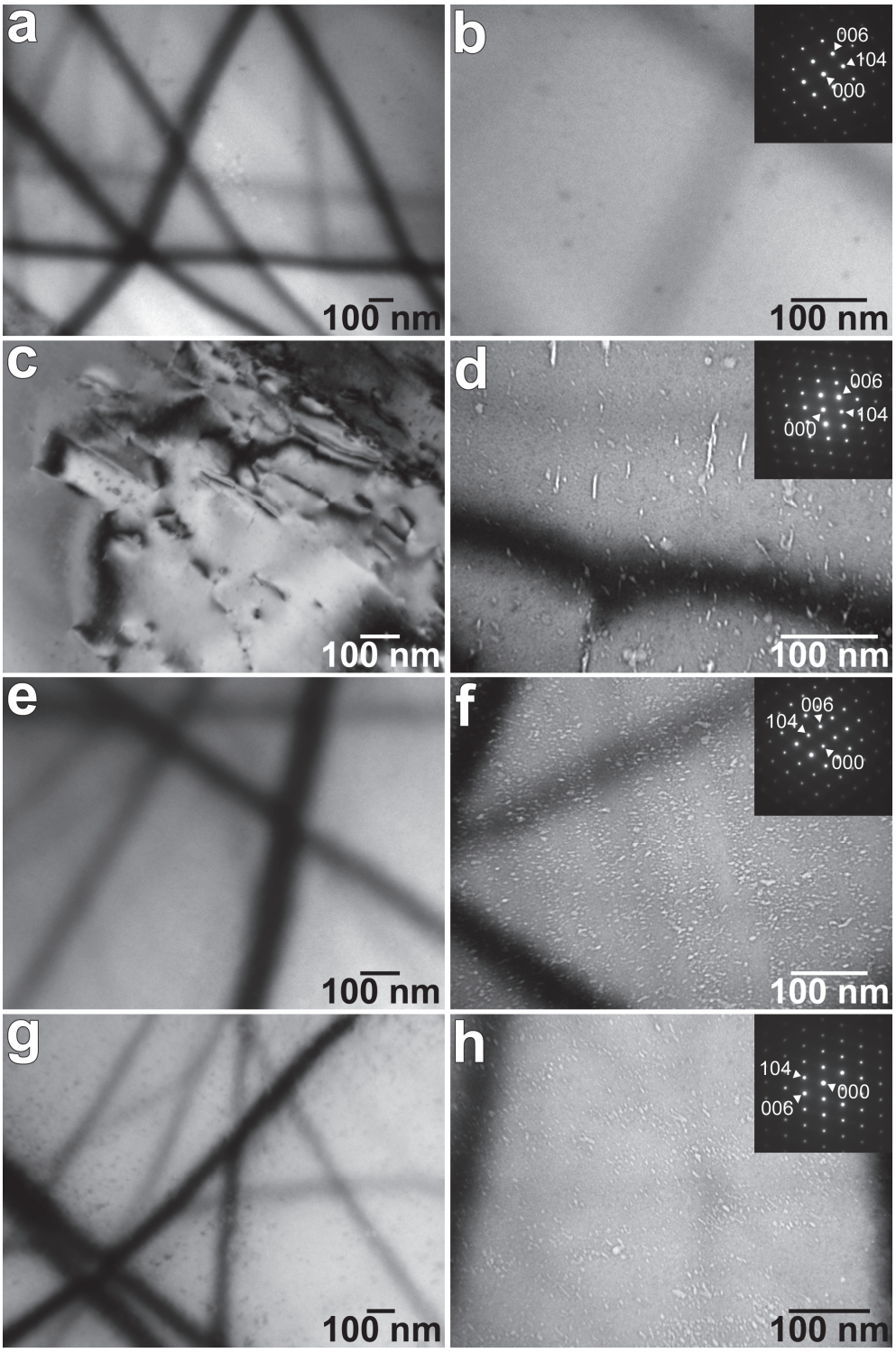

Figure 3–8. BF TEM images of the calcite crystals synthesized without additives (a,b), with soluble OMs extracted from *Pinctada* (c,d) and from *Atrina* (e,f), and with PANa (g,h). (a,c,e,g) were imaged with crystal orientation to form intense diffraction contrast and (b,d,f,h) were imaged with an under-focused condition. Electron diffraction patterns acquired are inserted.

observed in all specimens except the crystals without organic additives, indicating that the Fresnel contrasts correspond to the OMs added (Figure 3–8b, 8d, 8f and 8h). The OMs extracted from *Pinctada* are larger than those from *Atrina* and PANa, showing that they may be likely to form aggregates. Furthermore the shapes of the OMs are not spheres but ellipsoids elongated to particular directions. The elongated directions appear to be along {104} or {001} planes of calcite when the corresponding diffraction patterns are considered, but detailed three-dimensional analysis is needed to conclude it.

3.3.3 STEM–EELS analysis

The Fresnel contrasts in the crystals synthesized with the OMs from *Pinctada* were analyzed also using EELS in the same way as described in Chapter 2A (Figure 3–9). The Fresnel contrasts were recognized as dark contrasts in HAADF–STEM images. Compared with the spectrum obtained from only calcite crystals (black line), that from the dark contrasts in HAADF–STEM images (red line) shows the 289 eV peak with a shoulder at the lower energy-loss side, indicating the existence of the 284 eV peak,

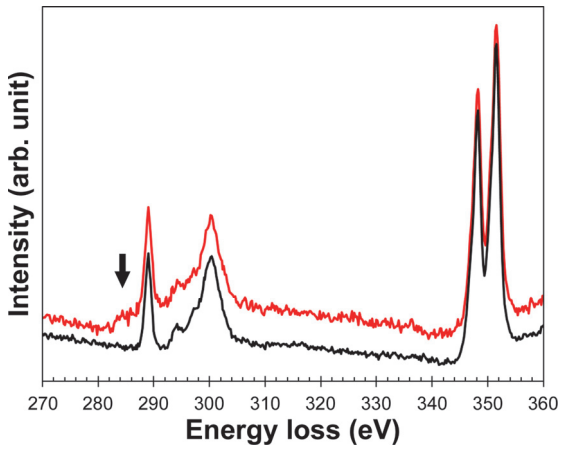

Figure 3–9. EELS spectra acquired from the calcite crystals synthesized with soluble OMs extracted from *Pinctada*. Black spectrum acquired from only calcite crystals, and red one from the dark contrasts in HAADF–STEM images or the Fresnel contrasts in under-focused TEM images. Arrow indicates the location of the 284 eV peak.

namely the organic additives inside the crystals. Thus it is concluded that the Fresnel contrasts in under-focused TEM images correspond to OMs incorporated into crystals.

3.3.4 XRD analysis

XRD analyses were also conducted for the synthesized calcite crystals (Figure 3–10). The crystals precipitated in the solution, not on the SAMs, were used for XRD measurements because the amount of those precipitated on the SAMs was too small. The local lattice strain along the a_i-axes is not distinct among all synthetic calcite crystals because the slopes of the regression lines are similar (Figure 3–10b). On the contrary, the local lattice strain along the *c*-axis is the largest for the crystals with the OMs from *Pinctada*, followed by those with the OMs from *Atrina* and with PANa (Figure 3–10a). This tendency is comparable to the biogenic calcite, although the

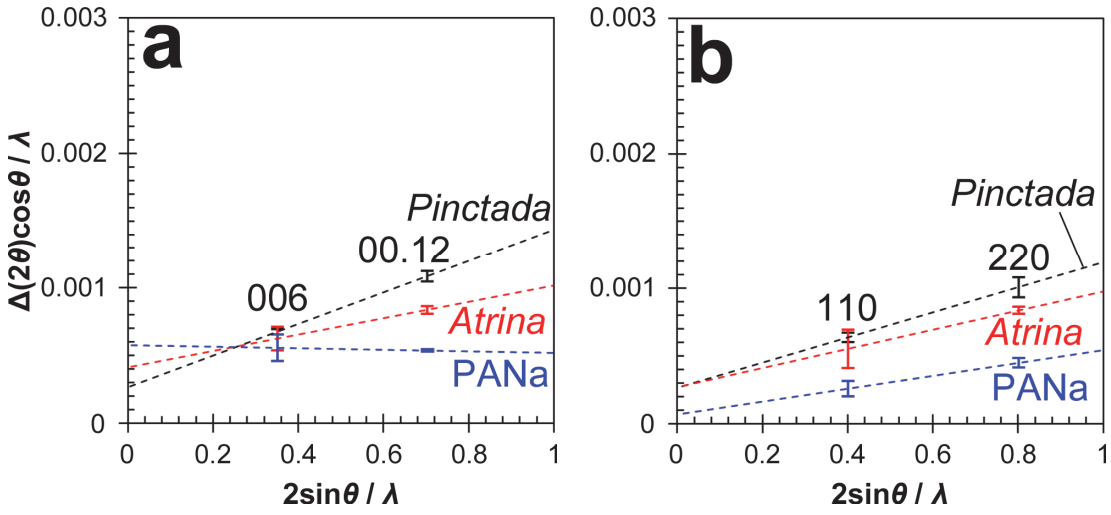

Figure 3–10. Williamson–Hall plots of the calcite crystals synthesized in the presence of soluble OMs extracted from *Pinctada* and *Atrina*, and PANa for the 006 and 00.12 (a), 110 and 220 (b) peaks in XRD profiles.

difference between the synthetic specimens is less distinct (see the results in Chapter 2A). These results indicate that the soluble OMs from *Pinctada* can induce more local lattice strain, and consequently make the calcite crystals crystallographically less perfect. This crystallographic imperfection possibly leads to the formation of sub-grains divided by small-angle misorientation in the prisms of *Pinctada*. It is noteworthy that PANa has the least significant influence on calcite crystal structure in spite of its negative charge. All of the y-intercept is smaller than 0.001 $Å^{-1}$, which corresponds to the coherence length of 94 nm, therefore the coherence length is larger than 94 nm. Since the limit for estimating the coherence length from the peak width of XRD profiles is approximately 100 nm as described in Chapter 2A, the accurate coherence length was not obtained here.

3.3.5 Amino acid composition analysis

Finally, I analyzed the amino acid compositions of the intracrystalline OMs that were extracted from the prisms of *Pinctada* and *Atrina* (Figure 3–11). Since both of the OMs contain a large amount of Asx (Asn and Asp), most proteins in the OMs are probably negatively charged. It is noteworthy that approximately a half of the amino acids (45.6 residue %) in the OMs from *Atrina* is composed of Asx, indicating that the OMs from *Atrina* are much more negatively charged than those from *Pinctada*. In addition, PANa, which was employed as an organic additive in the control synthetic experiments, is definitely a highly acidic polymer.

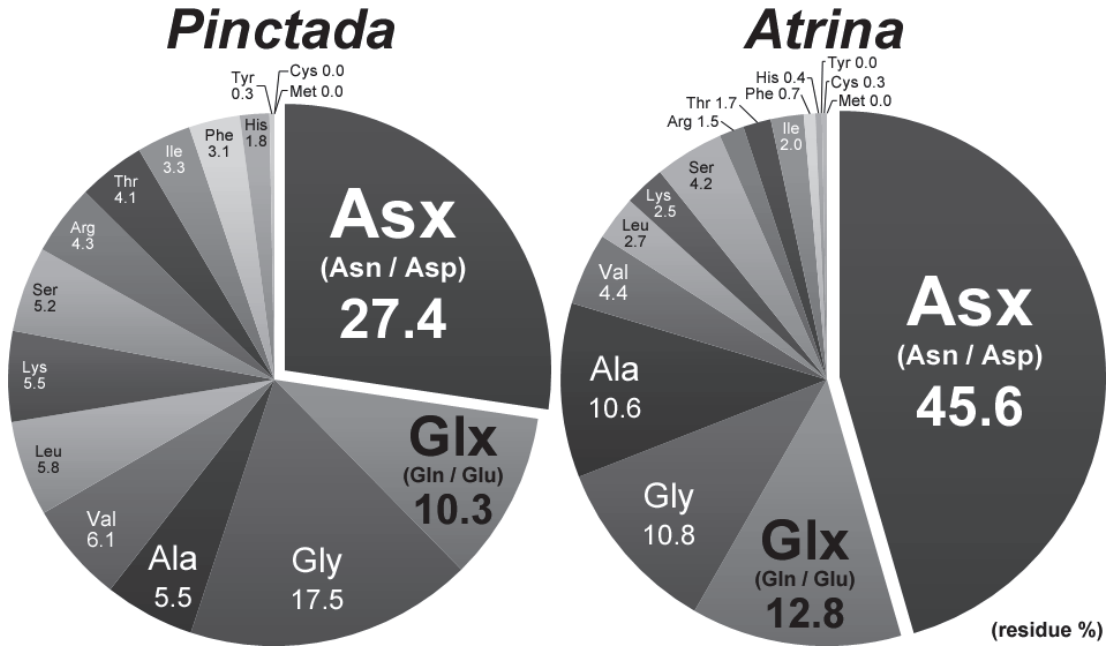

Figure 3–11. Amino acid compositions of soluble OMs extracted from the prisms of *Pinctada* and *Atrina*.

3.4 Discussion

In vitro synthetic experiments revealed that intracrystalline OMs extracted from the calcite prisms of *Pinctada* interact more strongly with calcite crystals, and consequently induce defective structure and lattice strain. On the other hand, resulting crystals became smaller when the OMs from *Atrina* and PANa were added to the *in vitro* setup, indicating that negatively charged OMs delay crystal growth. However, they have little influence on the crystal structure, which exhibited a perfect single-crystalline feature. These results are comparable with the defect-rich/free structure in the prisms of *Pinctada*/*Atrina*, implying that soluble OMs are one of the causes for constructing such

microstructures. In addition, the OMs extracted from *Pinctada* can interact more intimately with calcite crystals than more negatively charged OMs such as PANa, which means that other factors than the negative charge are responsible for the interaction.

Recently Kim et al. (2011) also reported that the OMs incorporated into crystals become ellipsoidal shapes. In their study, originally spherical shaped copolymer micelles changed to show oval cross-sections inside the crystals. Such shape change of the OMs occurs probably because the OMs effectively interact with the specific crystallographic planes of calcite. Although the original shapes of OMs added in this study are unknown, they may also interact with some particular planes more strongly because the OMs showed ellipsoidal shapes inside the crystals and were elongated along almost the same directions. Investigating the elongated directions of the OMs may lead to deep understanding of the mechanism by which the OMs are incorporated into crystals.

The defective structure in the prisms of *Pinctada* was reproduced by EDTA-soluble OMs in this study. Such structure has not been produced yet using only insoluble OMs. In many cases, defect-free single crystals were grown in a hydrogel of insoluble OMs owing to reduction of nucleation rate and suppression of ion diffusion. For example, Oaki et al. (2007) formed calcite crystals inside an agar gel, which are composed of apparent sub-units of several tens nanometers but show a complete single-crystalline feature. Furthermore the crystals retain a single-crystalline character even though the amount of insoluble OMs inside crystals become larger by increasing the concentration of the hydrogel. Whereas Grassmann et al. (2003) used a poly-acrylamide gel for producing calcite crystals with microstructures that consist of highly aligned crystallites of submicrometers. The characters of the crystals are similar

to those of microstructures in the prisms of *Pinctada*. Nevertheless the adjacent crystallites do not connect coherently, and the whole crystal holds large orientation spread. Thus insoluble OMs cannot induce microstructures with gradual orientation change in biogenic calcite. The interaction between soluble and insoluble OMs may be essential to create the crystals that are composed of sub-grains of several hundred nanometers divided by small-angle misorientation.

Although soluble OMs do induce defective structure in crystals, the amount of local lattice strain is rather smaller than that in biogenic crystals as shown in Williamson–Hall plots obtained using XRD measurements. Hence the microstructures in biogenic calcite may be reproduced more accurately by mutual influence of soluble and insoluble OMs.

3.5 Conclusions

The defect-rich calcite crystals in the prisms of *Pinctada* were reproduced to some extent *in vitro* by adding the intracrystalline OMs extracted from the prisms, whereas defect-free single crystals were formed even though the OMs from the prisms of *Atrina* and PANa were incorporated into the crystals. Since the OMs from *Atrina* and PANa are more negatively charged than those from *Pinctada*, the negative charge does not directly mean strong affinity for calcite crystals. These results indicate that certain soluble OMs have the responsibility to modify crystal structure and form distinctive microstructures in biominerals, which has been often advocated to date but scarcely demonstrated experimentally. This study suggests that the interaction between soluble OMs and

crystals definitely plays an important role in forming characteristic microstructures in biogenic calcite. Eventually harmonious relationships between soluble/insoluble OMs and crystals generate elaborate structure in biominerals.

Chapter 4.

Summary and general conclusions

This study focused on intracrystalline OMs in biominerals and aimed to reveal the interaction between crystals and the OMs. To work toward this goal, I investigated the calcite crystals constituting the outer layers of mollusk shells even at a nanoscale, and deliberated upon the functions of organic phases inside crystalline phases. The visualization of intracrystalline OMs by combining various electron microscopic analyses enabled me to examine the distribution and shapes of the OMs, and their spatial relationships with crystals. The outcome indicated that intracrystalline OMs include the OMs with thin reticulate form and those soluble in EDTA, which individually play distinct roles in biomineralization. The following is the summary of the results obtained in this study.

First, the detailed investigation and comparison of the calcite prismatic layers in *Pinctada* with those in *Atrina* were conducted. The prisms of *Pinctada* contain membranous and net-like OMs, which are distributed apparently inhomogeneously inside the crystals. Small-angle misorientation is generated at the locations of the OMs. As a result, the crystals are composed of sub-grains accompanying gradual orientation change and a large amount of lattice strain. OMs also exist inside the prisms of *Atrina*, but their shapes are thin fibers, which exhibit seeming homogeneous distribution in TEM observation. Since the thin fibrous OMs in *Atrina* have little influence on crystal structure unlike those in *Pinctada*, the prisms are defect-free single crystals.

The calcite crystals constituting the outer layers in *Pteria* and *Crassostrea* of bivalves, and *Haliotis* and *Collisella* of gastropods have similar microstructures to the defect-rich structure in the prisms of *Pinctada*. The crystal defects are induced by reticulate OMs also in these shells, implying that the constitution is a common character in diverse mollusk shells. The gradual orientation change originated from the defects

improves mechanical properties of the biogenic calcite by inhibiting propagation of cleavages along {104} planes. Thus it is reasonably concluded that organisms create defect-rich structure in the skeletons for protecting their soft bodies.

Although it is generally accepted that the reticulate OMs adjust crystal nucleation and growth rates and suppress ion diffusion by supplying environment for crystallization, they do not have influence on crystal structure. In fact, calcite crystals with defective structure have not been duplicated even though the crystals include the reticulate OMs. Whereas many previous studies demonstrated that OMs soluble in acid and/or EDTA are capable of affecting crystal structure. Hence I examined the influence of the OMs extracted by EDTA from the prisms of *Pinctada* and *Atrina* on crystal structure. Intracrystalline OMs extracted from these shells were added to the calcium-containing solution for *in vitro* crystallization. Defective structure was induced in the resulting calcite crystals that were synthesized in the presence of the EDTA-soluble OMs from *Pinctada*, but in contrast, those from *Atrina* did not influence on crystal structure. This synthetic experiment evidenced that EDTA-soluble OMs participate in the formation of defect-rich structure in the prisms of *Pinctada*. Nevertheless the synthesized crystals hold fairly smaller amount of strain than actual calcite prisms of *Pinctada*. Therefore I assert that the defect-rich structure in biogenic calcite is yielded by mutual influence of both reticulate and EDTA-soluble OMs. Some identified proteins that are included in mollusk shells actually have an ability to bind to the reticulate OMs such as chitin (Suzuki et al., 2004; Suzuki and Nagasawa, 2007; Suzuki et al., 2009).

On the basis of the results obtained in this study, I propose the following mechanism by which intracrystalline OMs regulate the microstructure of calcite crystals

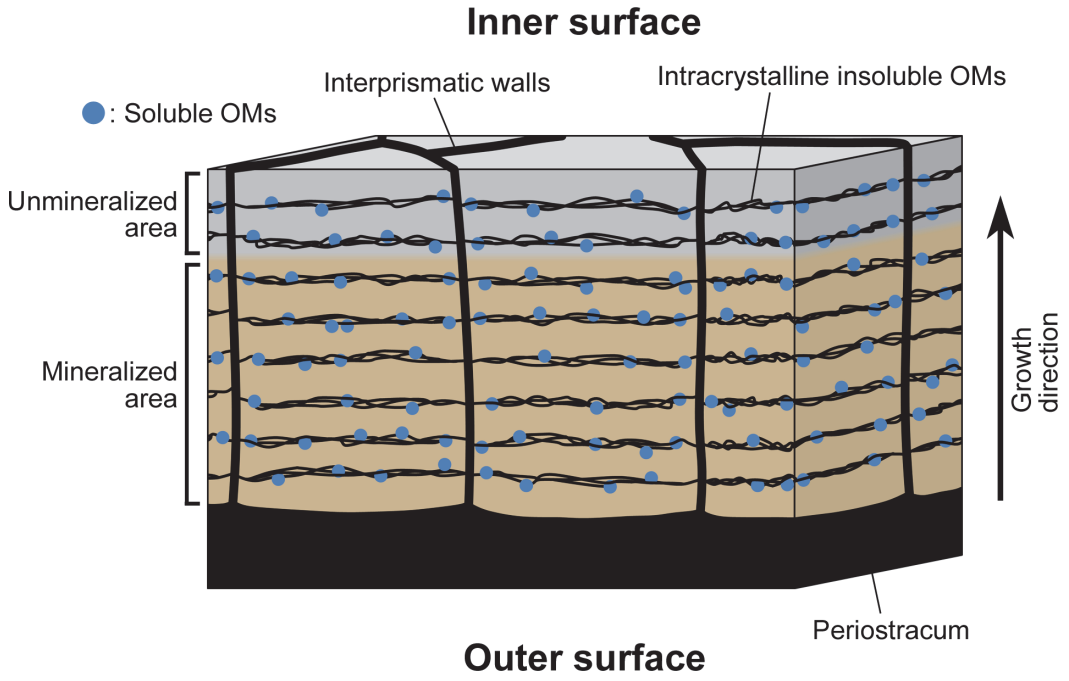

Figure 4–1. Schematic illustration of the prismatic structure, showing the mechanism by which intracrystalline OMs regulate the microstructure of calcite crystals constituting outer layers of mollusk shells.

constituting outer layers of mollusk shells (Figure 4–1).

1. An organic framework is constructed by OMs which include intercrystalline OMs and subsequent intracrystalline OMs with thin reticulate form. Another kind of OMs soluble in EDTA binds the reticulate OMs.
2. As the calcite crystals interact with EDTA-soluble OMs bound to the reticulate OMs, they grow inside the intercrystalline OMs, penetrating the reticulate OMs.

3. These intracrystalline OMs are incorporated into the crystals and build sub-grain microstructures with small-angle misorientation and defect-rich boundaries, which improve the mechanical properties of biogenic calcite by inhibiting propagation of cleavages.

In materials science, for instance, ceramics are stiff but brittle. Nevertheless the brittleness is conquered by decreasing crystallite size and controlling the density of grain boundaries. The grain boundaries block the propagation of cracks across crystallites. Such phenomenon may occur also in the defect-rich structure in biogenic calcite. However, the mechanism for improving the mechanical properties in biogenic calcite must be investigated independently in more detail because the defects are small-angle misorientation generated by the incorporation of OMs into crystals. It is noteworthy here that a lot of energy is needed for the processes of making ceramic materials such as sintering, on the contrary, biominerals are costlessly created at ambient temperature and pressure. Thus understanding the formation mechanism of biominerals gives hints for manufacturing structural materials at low cost.

Future work is to produce crystals with microstructures more similar to biominerals by combining soluble OMs with reticulate OMs in synthetic *in vitro* experiments. *In vitro* crystallization enables us to grasp the whole of the biomineralization processes. Furthermore, it is ultimately necessary to verify whether biominerals are actually formed through the processes as stated above. For this purpose, *in situ* examination such as cryo-electron microscopy should be applied to biomineralization.

Acknowledgements

I am grateful to Prof. Toshihiro Kogure (Department of Earth and Planetary Science, Graduate School of Science, The University of Tokyo, Japan) whose comments and suggestions were of inestimable value for my study. I express my deep sense of gratitude to Prof. Hiroyuki Kagi (Geochemical Research Center, Graduate School of Science, The University of Tokyo, Japan) as my chief examiner, Prof. Takashi Murakami (Department of Earth and Planetary Science, Graduate School of Science, The University of Tokyo, Japan), Prof. Eiji Abe (Department of Materials Engineering, Graduate School of Engineering, The University of Tokyo, Japan), and Prof. Yoshio Takahashi (Department of Earth and Planetary Systems Science, Graduate School of Science, Hiroshima University, Japan) as my associate examiners for providing me a lot of useful advice. I am pleased to acknowledge the considerable assistance of Dr. Michio Suzuki (Department of Applied Biological Chemistry, Graduate School of Agricultural and Life Sciences, The University of Tokyo, Japan). The author wishes to thank Prof. Peter R. Buseck (7*M Research Group, Arizona State University, USA), Prof. Hiromichi Nagasawa (Department of Applied Biological Chemistry, Graduate School of Agricultural and Life Sciences, The University of Tokyo, Japan), and Prof. Yohei Suzuki (Department of Earth and Planetary Science, Graduate School of Science, The University of Tokyo, Japan) for their helpful advice. I also thank Mr. Koji Ichimura, Mrs. Eiko Fujii (Department of Earth and Planetary Science, Graduate School of Science, The University of Tokyo, Japan), and Dr. Hideo Satsu (Department of Applied Biological Chemistry, Graduate School of Agricultural and Life Sciences, The University of Tokyo, Japan) who contributed their experimental skills of SEM, XRD,

FIB, amino acid composition analysis, and so forth. Some helpful discussion with SES seminar members is gratefully acknowledged. I am also grateful to Dr. Hideo Aoki (Mie Prefecture Fisheries Research Institute, Japan), Mr. Shusaka Akera (TASAKI & Co., Ltd., Japan), and Prof. Keiju Okano (Department of Biotechnology, Faculty of Bioresource Sciences, Akita Prefectural University, Japan) for providing me the mollusk shells. Finally, I would like to express my heartfelt gratitude to my family.

References

Addadi, L., Raz, S., Weiner, S. (2003) Taking advantage of disorder: Amorphous calcium carbonate and its roles in biomineralization. *Adv. Mater.* **15**, 959–970.

Addadi, L., Joester, D., Nudelman, F., Weiner, S. (2006) Mollusk shell formation: A source of new concepts for understanding biomineralization processes. *Chem. Eur. J.* **12**, 981–987.

Aizenberg, J., Albeck, S., Weiner, S., Addadi, L. (1994) Crystal protein interactions studied by overgrowth of calcite on biogenic skeletal elements. *J. Cryst. Growth* **142**, 156–164.

Aizenberg, J., Hanson, J., Koetzle, T.F., Leiserowitz, L., Weiner, S., Addadi, L. (1995a) Biologically induced reduction in symmetry: a study of crystal texture of calcitic sponge spicules. *Chem. Eur. J.* **1**, 414–422.

Aizenberg, J., Hanson, J., Ilan, M., Leiserowitz, L., Koetzle, T.F., Addadi, L., Weiner, S. (1995b) Morphogenesis of calcitic sponge spicules: a role for specialized proteins interacting with growing crystals. *FASEB J.* **9**, 262–268.

Aizenberg, J., Hanson, J., Koetzle, T.F., Weiner, S., Addadi, L. (1997) Control of macromolecule distribution within synthetic and biogenic single calcite crystals. *J. Am. Chem. Soc.* **119**, 881–886.

Aizenberg, J., Black, A.J., Whitesides, G.M. (1999a) Control of crystal nucleation by patterned self-assembled monolayers. *Nature* **398**, 495–498.

Aizenberg, J., Black, A.J., Whitesides, G.H. (1999b) Oriented growth of calcite controlled by self-assembled monolayers of functionalized alkanethiols supported on gold and silver. *J. Am. Chem. Soc.* **121**, 4500–4509.

Aizenberg, J., Tkachenko, A., Weiner, S., Addadi, L., Hendler, G. (2001) Calcitic microlenses as part of the photoreceptor system in brittlestars. *Nature* **412**, 819–822.

Albeck, S., Aizenberg, J., Addadi, L., Weiner, S. (1993) Interactions of various skeletal intracrystalline components with calcite crystals. *J. Am. Chem. Soc.* **115**, 11691–11697.

Albeck, S., Weiner, S., Addadi, L. (1996a) Polysaccharides of intracrystalline glycoproteins modulate calcite crystal growth in vitro. *Chem. Eur. J.* **2**, 278–284.

Albeck, S., Addadi, L., Weiner, S. (1996b) Regulation of calcite crystal morphology by intracrystalline acidic proteins and glycoproteins. *Connect. Tissue Res.* **35**, 365–370.

Asenath-Smith, E., Li, H., Keene, E.C., Seh, Z.W., Estroff, L.A. (2012) Crystal growth of calcium carbonate in hydrogels as a model of biomineralization. *Adv. Funct. Mater.* **22**, 2891–2914.

Bazylinski, D.A. (1996) Controlled biomineralization of magnetic minerals by magnetotactic bacteria. *Chem. Geol.* **132**, 191–198.

Bazylinski, D.A., Frankel, R.B. (2003) Biologically controlled mineralization in prokaryotes. *Biominer.* **54**, 217–247.

Belcher, A.M., Wu, X.H., Christensen, R.J., Hansma, P.K., Stucky, G.D., Morse, D.E. (1996) Control of crystal phase switching and orientation by soluble mollusc-shell proteins. *Nature* **381**, 56–58.

Bentov, S., Weil, S., Glazer, L., Sagi, A., Berman, A. (2010) Stabilization of amorphous calcium carbonate by phosphate rich organic matrix proteins and by single phosphoamino acids. *J. Struct. Biol.* **171**, 207–215.

Berman, A., Addadi, L., Weiner, S. (1988) Interactions of sea-urchin skeleton macromolecules with growing calcite crystals— a study of intracrystalline proteins.

Nature **331**, 546–548.

Berman, A., Hanson, J., Leiserowitz, L., Koetzle, T.F., Weiner, S., Addadi, L. (1993a) Biological control of crystal texture: a widespread strategy for adapting crystal properties to function. *Science* **259**, 776–779.

Berman, A., Hanson, J., Leiserowitz, L., Koetzle, T.F., Weiner, S., Addadi, L. (1993b) Crystal–protein interactions: controlled anisotropic changes in crystal microtexture. *J. Phys. Chem.* **97**, 5162–5170.

Bevelander, G., Nakahara, H. (1969) An electron microscope study of formation of nacreous layer in shell of certain bivalve molluscs. *Calcif. Tissue Res.* **3**, 84–92.

Borowitzka, M.A. (1982) Morphological and cytological aspects of algal calcification. *Int. Rev. Cytol.* **74**, 127–162.

Borukhin, S., Bloch, L., Radlauer, T., Hill, A.H., Fitch, A.N., Pokroy, B. (2012) Screening the incorporation of amino acids into an inorganic crystalline host: the case of calcite. *Adv. Funct. Mater.* **22**, 4216–4224.

Carter, J.G. (1980) Environmental and biological controls of bivalve shell mineralogy and microstructure, in: Rhoads D.C., Lutz R.A. (Eds.), Skeletal Growth of Aquatic Organisms, Plenum Press, New York, pp. 69–113.

Carter, J.G. (Ed.) (1990a) Skeletal Biomineralization: Patterns, Processes and Evolutionary Trends Volume 1. Van Nostrand Reinhold, New York.

Carter, J.G. (Ed.) (1990b) Skeletal Biomineralization: Patterns, Processes and Evolutionary Trends Volume 2. Atlas and Index. Van Nostrand Reinhold, New York.

Checa, A.G., Rodríguez-Navarro, A.B., Esteban-Delgado, F.J. (2005) The nature and formation of calcitic columnar prismatic shell layers in pteriomorphian bivalves.

Biomaterials **26**, 6404–6414.

Checa, A.G., Esteban-Delgado, F.J., Ramírez-Rico, J., Rodríguez-Navarro, A.B. (2009) Crystallographic reorganization of the calcitic prismatic layer of oysters. *J. Struct. Biol.* **167**, 261–270.

Checa, A.G., Bonarski, J.T., Willinger, M.G., Faryna, M., Berent, K., Kania, B., Gonzalez-Segura, A., Pina, C.M., Pospiech, J., Morawiec, A. (2013) Crystallographic orientation inhomogeneity and crystal splitting in biogenic calcite. *J. R. Soc. Interface* **10**, 20130425.

Cölfen, H., Mann, S. (2003) Higher-order organization by mesoscale self-assembly and transformation of hybrid nanostructures. *Angew. Chem. Int. Ed.* **42**, 2350–2365.

Currey, J.D. (1977) Mechanical properties of mother of pearl in tension. *Proc. R. Soc. Lond. B* **196**, 443–463.

Currey, J.D. (1999) The design of mineralised hard tissues for their mechanical functions. *J. Exp. Biol.* **202**, 3285–3294.

Dauphin, Y., Cuif, J.P., Doucet, J., Salomé, M., Susini, J., Williams, C.T. (2003a) In situ chemical speciation of sulfur in calcitic biominerals and the simple prism concept. *J. Struct. Biol.* **142**, 272–280.

Dauphin, Y., Cuif, J.P., Doucet, J., Salomé, M., Susini, J., Williams, C.T. (2003b) In situ mapping of growth lines in the calcitic prismatic layers of mollusc shells using X-ray absorption near-edge structure (XANES) spectroscopy at the sulphur K-edge. *Mar. Biol.* **142**, 299–304.

Dauphin, Y. (2003) Soluble organic matrices of the calcitic prismatic shell layers of two Pteriomorphid bivalves. *Pinna nobilis* and *Pinctada margaritifera*. *J. Biol. Chem.* **278**, 15168–15177.

Dauphin, Y., Cuif, J.P., Salomé, C., Susini, J. (2005) Speciation and distribution of sulfur in a mollusk shell as revealed by in situ maps using X-ray absorption near-edge structure (XANES) spectroscopy at the S *K*-edge. *Am. Mineral.* **90**, 1748–1758.

Dauphin, Y. (2006) Structure and composition of the septal nacreous layer of *Nautilus macromphalus* L. (Mollusca, Cephalopoda). *Zool.* **109**, 85–95.

Dauphin, Y. (2008) The nanostructural unity of Mollusc shells. *Mineral. Mag.* **72**, 243–246.

De Paula, S.M., Silveira, M. (2009) Studies on molluscan shells: Contributions from microscopic and analytical methods. *Micron* **40**, 669–690.

DeOliveira, D.B., Laursen, R.A. (1997) Control of calcite crystal morphology by a peptide designed to bind to a specific surface. *J. Am. Chem. Soc.* **119**, 10627–10631.

Didymus, J.M., Oliver, P., Mann, S., Devries, A.L., Hauschka, P.V., Westbroek, P. (1993) Influence of low-molecular-weight and macromolecular organic additives on the morphology of calcium carbonate. *J. Chem. Soc. Faraday Trans.* **89**, 2891–2900.

Dunin-Borkowski, R.E., McCartney, M.R., Frankel, R.B., Bazylinski, D.A., Pósfai, M., Buseck, P.R. (1998) Magnetic microstructure of magnetotactic bacteria by electron holography. *Science* **282**, 1868–1870.

Emlet, R.B. (1982) Echinoderm calcite: a mechanical analysis from larval spicules. *Biol. Bull.* **163**, 264–275.

Epstein, S., Buchsbaum, R., Lowenstam, H., Urey, H.C. (1951) Carbonate-water isotopic temperature scale. *Geol. Soc. Am. Bull.* **62**, 417–426.

Esteban-Delgado, F.J., Harper, E.M., Checa, A.G., Rodríguez-Navarro, A.B. (2008)

Origin and expansion of foliated microstructure in Pteriomorph bivalves. *Biol. Bull.* **214**, 153–165.

Falini, G., Albeck, S., Weiner, S., Addadi, L. (1996) Control of aragonite or calcite polymorphism by mollusk shell macromolecules. *Science* **271**, 67–69.

Fortin, D., Beveridge, T.J. (2000) Mechanistic routes towards biomineral surface development, in: Bäuerlein E. (Ed.), Biomineralisation: From Biology to Biotechnology and Medical Application, Wiley-VCH, Weinheim, pp. 7–24.

Franceschi, V.R., Nakata, P.A. (2005) Calcium oxalate in plants: Formation and function. *Ann. Rev. Plant Biol.* **56**, 41–71.

Frankel, R.B., Bazylinski, D.A. (2003) Biologically induced mineralization by bacteria. *Biominer.* **54**, 95–114.

Friedrich, H., McCartney, M.R., Buseck, P.R. (2005) Comparison of intensity distributions in tomograms from BF TEM, ADF STEM, HAADF STEM, and calculated tilt series. *Ultramicroscopy* **106**, 18–27.

Fuchigami, T., Sasaki, T. (2005) The shell structure of the Recent Patellogastropoda (Mollusca: Gastropoda). *Paleontol. Res.* **9**, 143–168.

Gordon, L.M., Joester, D. (2011) Nanoscale chemical tomography of buried organic–inorganic interfaces in the chiton tooth. *Nature* **469**, 194–197.

Grassman, O., Neder, R.B., Putnis, A., Löbmann, P. (2003) Biomimetic control of crystal assembly by growth in an organic hydrogel network. *Am. Mineral.* **88**, 647–652.

Grégoire, C. (1961) Structure of conchiolin cases of prisms in *Mytilus edulis* Linné. *J. Biophys. Biochem. Cytol.* **9**, 395–400.

Gries, K., Kröger, R., Kübel, C., Fritz, M., Rosenauer, A. (2009) Investigations of voids

in the aragonite platelets of nacre. *Acta Biomater.* **5**, 3038–3044.

Hall, W. (1949) X-ray line broadening in metals. *Proc. Phys. Soc. London Sect. A* **62**, 741–743.

Han, Y.J., Aizenberg, J. (2003) Face-selective nucleation of calcite on self-assembled monolayers of alkanethiols: Effect of the parity of the alkyl chain. *Angew. Chem. Int. Ed.* **42**, 3668–3670.

Hasse, B., Ehrenberg, H., Marxen, J.C., Becker, W., Epple, M. (2000) Calcium carbonate modifications in the mineralized shell of the freshwater snail *Biomphalaria glabrata*. *Chem. Eur. J.* **6**, 3679–3685.

Hedegaard, C. (1997) Shell structures of the recent Vetigastropoda. *J. Molluscan Stud.* **63**, 369–377.

Hendriks, I.E., Basso, L., Deudero, S., Cabanellas-Reboredo, M., Álvarez, E. (2012) Relative growth rates of the noble pen shell *Pinna nobilis* throughout ontogeny around the Balearic Islands (Western Mediterranean, Spain). *J. Shellfish Res.* **31**, 749–756.

Hickman, C.S. (2004) The problem of similarity: analysis of repeated patterns of microsculpture on gastropod larval shells. *Invertebr. Biol.* **123**, 198–211.

Hofmann, H.J., Masson, M. (1994) Archean stromatolites from Abitibi greenstone belt, Quebec, Canada. *Geol. Soc. Am. Bull.* **106**, 424–429.

Jackson, A.P., Vincent, J.F.V., Turner, R.M. (1988) The mechanical design of nacre. *Proc. R. Soc. Lond. B* **234**, 415–440.

Kamat, S., Su, X., Ballarini, R., Heuer, A.H. (2000) Structural basis for the fracture toughness of the shell of the conch *Strombus gigas*. *Nature* **405**, 1036–1040.

Kaplan, D.L. (1998) Mollusc shell structures: novel design strategies for synthetic

materials. *Curr. Opin. Solid State Mater. Sci.* **3**, 232–236.

Kelly, T.F., Miller, M.K. (2007) Invited review article: Atom probe tomography. *Rev. Sci. Instrum.* **78**, 031101.

Kennedy, W.J., Taylor, J.D., Hall, A. (1969) Environmental and biological controls on bivalve shell mineralogy. *Biol. Rev.* **44**, 499–530.

Kim, Y.Y., Ganesan, K., Yang, P., Kulak, A.N., Borukhin, S., Pechook, S., Ribeiro, L., Kröeger, R., Eichhorn, S.J., Armes, S.P., Pokroy, B., Meldrum, F.C. (2011) An artificial biomineral formed by incorporation of copolymer micelles in calcite crystals. *Nat. Mater.* **10**, 890–896.

Kunitake, M.E., Mangano, L.M., Peloquin, J.M., Baker, S.P., Estroff, L.A. (2013) Evaluation of strengthening mechanisms in calcite single crystals from mollusk shells. *Acta Biomater.* **9**, 5353–5359.

Li, H., Estroff, L.A. (2009) Calcite growth in hydrogels: assessing the mechanism of polymer-network incorporation into single crystals. *Adv. Mater.* **21**, 470–473.

Li, H., Xin, H.L., Muller, D.A., Estroff, L.A. (2009) Visualizing the 3D internal structure of calcite single crystals grown in agarose hydrogels. *Science* **326**, 1244–1247.

Li, H., Xin, H.L., Kunitake, M.E., Keene, E.C., Muller, D.A., Estroff, L.A. (2011) Calcite prisms from mollusk shells (*Atrina rigida*): swiss-cheese-like organic–inorganic single-crystal composites. *Adv. Funct. Mater.* **21**, 2028–2034.

Lowenstam, H.A. (1981) Minerals formed by organisms. *Science* **211**, 1126–1131.

Lowenstam, H.A. (1964) Sr/Ca ratio of skeletal aragonites from the recent marine biota at Palau and from fossil gastropods, in: Craig H., Miller S.L., Wasserburg G.J. (Eds.), Isotopic and Cosmic Chemistry, North-Holland, Amsterdam, pp. 114–132.

Luquet, G., Marin, F. (2004) Biomineralisations in crustaceans: storage strategies. *C. R. Palevol* **3**, 515–534.

Lutts, A., Grandjean, J., Grégoire, C. (1960) X-ray diffraction patterns from the prisms of mollusk shells. *Arch. Int. Physiol. Biochim.* **68**, 829–831.

MacDonald, J., Freer, A., Cusack, M. (2010) Alignment of crystallographic *c*-axis throughout the four distinct microstructural layers of the oyster *Crassostrea gigas*. *Cryst. Growth Des.* **10**, 1243–1246.

Mann, S., Parker, S.B., Ross, M.D., Skarnulis, A.J., Williams, R.J.P. (1983) The ultrastructure of the calcium carbonate balance organs of the inner ear: an ultra-high resolution electron microscopy study. *Proc. R. Soc. Lond. B* **218**, 415–424.

Mann, S., Didymus, J.M., Sanderson, N.P., Heywood, B.R., Samper, E.J.A. (1990) Morphological influence of functionalized and non-functionalized-α,ω-dicarboxylates on calcite crystallization. *J. Chem. Soc. Faraday Trans.* **86**, 1873–1880.

Mann, S. (1993) Molecular tectonics in biomineralization and biomimetic materials chemistry. *Nature* **365**, 499–505.

Mann, S. (2001) Biomineralization Principles and Concepts in Bioinorganic Materials Chemistry. Oxford University Press, Oxford.

Mansot, J.L., Golabkan, V., Romana, L., Césaire, T. (2003) Chemical and physical characterization by EELS of strontium hexanoate reverse micelles and strontium carbonate nanophase produced during tribological experiments. *J. Microsc.* **210**, 110–118.

Marin, F., Luquet, G. (2004) Molluscan shell proteins. *C. R. Palevol* **3**, 469–492.

Martin, J.M., Mansot, J.L., Hallouis, M. (1989) Energy filtered electron microscopy

(EFEM) of overbased reverse micelles. *Ultramicroscopy* **30**, 321–327.

Martin, J.M., Vacher, B., Ponsonnet, L., Dupuis, V. (1996) Chemical bond mapping of carbon by image-spectrum EELS in the second derivative mode. *Ultramicroscopy* **65**, 229–238.

Marxen, J.C., Hammer, M., Gehrke, T., Becker, W. (1998) Carbohydrates of the organic shell matrix and the shell-forming tissue of the snail *Biomphalaria glabrata* (Say). *Biol. Bull.* **194**, 231–240.

Meldrum, F.C. (2003) Calcium carbonate in biomineralisation and biomimetic chemistry. *Int. Mater. Rev.* **48**, 187–224.

Nakahara, H. (1979) An electron microscope study of the growing surface of nacre in two gastropod species, *Turbo cornutus* and *Tegula pfeifferi*. *Venus* **38**, 205–211.

Nudelman, F., Gotliv, B.A., Addadi, L., Weiner, S. (2006) Mollusk shell formation: Mapping the distribution of organic matrix components underlying a single aragonitic tablet in nacre. *J. Struct. Biol.* **153**, 176–187.

Nudelman, F., Chen, H.H., Goldberg, H.A., Weiner, S., Addadi, L. (2007) Spiers memorial lecture: lessons from biomineralization: comparing the growth strategies of mollusc shell prismatic and nacreous layers in *Atrina rigida*. *Faraday Discuss.* **136**, 9–25.

Oaki, Y., Hayashi, S., Imai, H. (2007) A hierarchical self-similar structure of oriented calcite with association of an agar gel matrix: inheritance of crystal habit from nanoscale. *Chem. Commun.*, 2841–2843.

Okumura, T., Suzuki, M., Nagasawa, H., Kogure, T. (2010) Characteristics of biogenic calcite in the prismatic layer of a pearl oyster, *Pinctada fucata*. *Micron* **41**, 821–826.

Okumura, T., Suzuki, M., Nagasawa, H., Kogure, T. (2012) Microstructural variation of

biogenic calcite with intracrystalline organic macromolecules. *Cryst. Growth Des.* **12**, 224–230.

Olson, I.C., Metzler, R.A., Tamura, N., Kunz, M., Killian, C.E., Gilbert, P.U.P.A. (2013) Crystal lattice tilting in prismatic calcite. *J. Struct. Biol.* **183**, 180–190.

Paasche, E. (2002) A review of the coccolithophorid *Emiliania huxleyi* (Prymnesiophyceae), with particular reference to growth, coccolith formation, and calcification–photosynthesis interactions. *Phycol.* **40**, 503–529.

Palmer, A.R. (1992) Calcification in marine molluscs: How costly is it?. *Proc. Natl. Acad. Sci. USA* **89**, 1379–1382.

Pennycook S.J., Nellist P.D. (Eds.) (2011) Scanning Transmission Electron Microscopy: Imaging and Analysis. Springer, New York.

Pokroy, B., Fitch, A.N., Marin, F., Kapon, M., Adir, N., Zolotoyabko, E. (2006a) Anisotropic lattice distortions in biogenic calcite induced by intra-crystalline organic molecules. *J. Struct. Biol.* **155**, 96–103.

Pokroy, B., Fitch, A.N., Zolotoyabko, E. (2006b) The microstructure of biogenic calcite: A view by high-resolution synchrotron powder diffraction. *Adv. Mater.* **18**, 2363–2368.

Robach, J.S., Stock, S.R., Veis, A. (2005) Transmission electron microscopy characterization of macromolecular domain cavities and microstructure of single-crystal calcite tooth plates of the sea urchin *Lytechinus variegatus*. *J. Struct. Biol.* **151**, 18–29.

Sato, A., Nagasaka, S., Furihata, K., Nagata, S., Arai, I., Saruwatari, K., Kogure, T., Sakuda, S., Nagasawa, H. (2011) Glycolytic intermediates induce amorphous calcium carbonate formation in crustaceans. *Nat. Chem. Biol.* **7**, 197–199.

Schrag, D.P., Linsley, B.K. (2002) Paleoclimate: Corals, chemistry, and climate. *Science* **296**, 277–278.

Schüler, D., Frankel, R.B. (1999) Bacterial magnetosomes: microbiology, biomineralization and biotechnological applications. *Appl. Microbiol. Biotechnol.* **52**, 464–473.

Silina, A.V. (2012) Growth of bivalve *Atrina vexillum* in the gulf of Thailand. *J. Shellfish Res.* **31**, 989–995.

Song, R.Q., Cölfen, H. (2011) Additive controlled crystallization. *Crystengcomm* **13**, 1249–1276.

Suzuki, M., Murayama, E., Inoue, H., Ozaki, N., Tohse, H., Kogure, T., Nagasawa, H. (2004) Characterization of Prismalin-14, a novel matrix protein from the prismatic layer of the Japanese pearl oyster (*Pinctada fucata*). *Biochem. J.* **382**, 205–213.

Suzuki, M., Nagasawa, H. (2007) The structure–function relationship analysis of Prismalin-14 from the prismatic layer of the Japanese pearl oyster, *Pinctada fucata*. *FEBS J.* **274**, 5158–5166.

Suzuki, M., Saruwatari, K., Kogure, T., Yamamoto, Y., Nishimura, T., Kato, T., Nagasawa, H. (2009) An acidic matrix protein, Pif, is a key macromolecule for nacre formation. *Science* **325**, 1388–1390.

Suzuki, M., Kameda, J., Sasaki, T., Saruwatari, K., Nagasawa, H., Kogure, T. (2010) Characterization of the multilayered shell of a limpet, *Lottia kogamogai* (Mollusca: Patellogastropoda), using SEM–EBSD and FIB–TEM techniques. *J. Struct. Biol.* **171**, 223–230.

Suzuki, M., Okumura, T., Nagasawa, H., Kogure, T. (2011) Localization of intracrystalline organic macromolecules in mollusk shells. *J. Cryst. Growth* **337**,

24–29.

Tao, J., Zhou, D., Zhang, Z., Xu, X., Tang, R. (2009) Magnesium-aspartate-based crystallization switch inspired from shell molt of crustacean. *Proc. Natl. Acad. Sci. USA* **106**, 22096–22101.

Taylor, J.D., Kennedy, W.J., Hall, A. (1969) The shell structure and mineralogy of the Bivalvia. Introduction. Nuculacea–Trigonacea. *Bull. Br. Mus. (Nat. Hist.) Zool. Suppl.* **3**, 1–125.

Taylor, J.D., Reid, D.G. (1990) Shell microstructure and mineralogy of the Littorinidae: ecological and evolutionary significance. *Hydrobiol.* **193**, 199–215.

Tong, H., Hu, J.M., Ma, W.T., Zhong, G.R., Yao, S.N., Cao, N.X. (2002) In situ analysis of the organic framework in the prismatic layer of mollusc shell. *Biomaterials* **23**, 2593–2598.

Towe, K.M., Thompson, G.R. (1972) Structure of some bivalve shell carbonates prepared by ion-beam thinning. A comparison study. *Calcif. Tissue Res.* **10**, 38–48.

Travaille, A.M., Donners, J.J.J.M., Gerritsen, J.W., Sommerdijk, N.A.J.M., Nolte, R.J.M., van Kempen, H. (2002) Aligned growth of calcite crystals on a self-assembled monolayer. *Adv. Mater.* **14**, 492–495.

Travaille, A.M., Kaptijn, L., Verwer, P., Hulsken, B., Elemans, J.A.A.W., Nolte, R.J.M., van Kempen, H. (2003) Highly oriented self-assembled monolayers as templates for epitaxial calcite growth. *J. Am. Chem. Soc.* **125**, 11571–11577.

Tsujii, T., Sharp, D.G., Wilbur, K.M. (1958) Studies on shell formation 7. The submicroscopic structure of the shell of the oyster *Crassostrea virginica*. *J. Biophys. Biochem. Cytol.* **4**, 275–287.

Tsukamoto, D., Sarashina, I., Endo, K. (2004) Structure and expression of an unusually

acidic matrix protein of pearl oyster shells. *Biochem. Biophys. Res. Commun.* **320**, 1175–1180.

Urey, H.C., Lowenstam, H.A., Epstein, S., McKinney, C.R. (1951) Measurement of paleotemperatures and temperatures of the upper cretaceous of England, Denmark, and the southeastern United States. *Geol. Soc. Am. Bull.* **62**, 399–416.

Van Cappellen, P. (2003) Biomineralization and global biogeochemical cycles. *Rev. Mineral. Geochem.* **54**, 357–381.

Van Poppel, L.H., Friedrich, H., Spinsby, J., Chung, S.H., Seinfeld, J.H., Buseck, P.R. (2005) Electron tomography of nanoparticle clusters: Implications for atmospheric lifetimes and radiative forcing of soot. *Geophys. Res. Lett.* **32**, L24811.

Varlot, K., Martin, J.M., Quet, C., Kihn, Y.. (1997) Towards sub-nanometer scale EELS analysis of polymers in the TEM. *Ultramicroscopy* **68**, 123–133.

Varlot, K., Martin, J.M., Gonbeau, D., Quet, C. (1999) Chemical bonding analysis of electron-sensitive polymers by EELS. *Polymer* **40**, 5691–5697.

Velázquez-Castillo, R.R., Reyes-Gasga, J., García-Gutierrez, D.I., Jose-Yacaman, M. (2006) Crystal structure characterization of nautilus shell at different length scales. *Biomaterials* **27**, 4508–4517.

Wada, K. (1961) Crystal growth of molluscan shells. *Bull. Natl. Pearl Res. Lab.* **7**, 703–828.

Wang, R.Z., Addadi, L., Weiner, S. (1997) Design strategies of sea urchin teeth: Structure, composition and micromechanical relations to function. *Phil. Trans. R. Soc. Lond. B* **352**, 469–480.

Warren, B.E. (1941) X-ray diffraction methods. *J. Appl. Phys.* **12**, 375–384.

Watabe, N., Wada, K. (1956) On the shell structures of Japanese pearl oyster, *Pinctada*

martensii (Dunker). (I) Prismatic layer I.. *Rep. Fac. Fish. Prefect. Univ. Mie* **2**, 227–235.

Watabe, N., Wilbur, K.M. (1961) Studies on shell formation 9. An electron microscope study of crystal layer formation in oyster. *J. Biophys. Biochem. Cytol.* **9**, 761–771.

Weiner, S. (1979) Aspartic acid-rich proteins: Major components of the soluble organic matrix of mollusk shells. *Calcif. Tissue Int.* **29**, 163–167.

Weiner, S., Traub, W. (1980) X-ray diffraction study of the insoluble organic matrix of mollusk shells. *FEBS Lett.* **111**, 311–316.

Weiner, S., Addadi, L. (1997) Design strategies in mineralized biological materials. *J. Mater. Chem.* **7**, 689–702.

Weiner, S., Addadi, L. (2002) At the cutting edge. *Science* **298**, 375–376.

Weiner, S., Dove, P.M. (2003) An overview of biomineralization processes and the problem of the vital effect. *Biominer.* **54**, 1–29.

Weiss, I.M., Renner, C., Strigl, M.G., Fritz, M. (2002) A simple and reliable method for the determination and localization of chitin in abalone nacre. *Chem. Mater.* **14**, 3252–3259.

Weiss, I.M., Schönitzer, V. (2006) The distribution of chitin in larval shells of the bivalve mollusk *Mytilus galloprovincialis*. *J. Struct. Biol.* **153**, 264–277.

Williams D.B., Carter C.B. (Eds.) (2009) Transmission Electron Microscopy: A Textbook for Materials Science. Springer, New York.

Williamson, G.K., Hall, W.H. (1953) X-ray line broadening from filed aluminium and wolfram. *Acta Metall.* **1**, 22–31.

Wise, S.W. (1970) Microarchitecture and deposition of gastropod nacre. *Science* **167**, 1486–1488.

Younis, S., Kauffmann, Y., Bloch, L., Zolotoyabko, E. (2012) Inhomogeneity of nacre lamellae on the nanometer length scale. *Cryst. Growth Des.* **12**, 4574–4579.

堀内繁雄（1988）「高分解能電子顕微鏡　−原理と利用法−」共立出版株式会社, 東京